www.czasopisma.pan.pl PAN POLSKA AKADEMIA NAUK www.journals.pan.pl

Arch. Metall. Mater. **63** (2018), 1, 445-450

DOI: 10.24425/118959

Q. YUAN*,**, G.XU*,**#, M. ZHOU*,**, B. HE*,**, H. HU*,**

COMBINED INFLUENCE OF SILICON CONTENT AND OXYGEN CONCENTRATION ON THE OXIDATION PROCESS OF SILICON-CONTAINING STEELS

The combined influence of silicon content and oxygen concentration on silicon-containing steels was investigated, via a heating route similar to that applied in the industrial reheating process, using a Simultaneous Thermal Analyzer (STA). Four different oxygen concentrations and three different isothermal holding times were designed. The results show that the effect of silicon on the mass gain depends on the oxygen concentration and the oxidation time. The mass gain of low-silicon steel is greater than that of high-silicon steel at 1260°C in the oxygen concentrations of 1.0 vol.% and 2.0 vol.%, even when the isothermal holding time is 90 minutes. However, there is a critical time point for mass gain in oxygen concentrations ≥3.0 vol.%. The mass gain of low-silicon steel is greater before and smaller after this critical point. The critical time is deferred with decreasing oxygen concentration.

Keywords: silicon content, oxygen concentration, mass gain, isothermal holding time

1. Introduction

Red scale as a serious surface defect that often appears in silicon-containing steels [1-5]. The formation mechanism of red scale has been reported by Okada [6] and Fukagawa [7,8]. At first, silicon reacts with oxygen diffusing into steel and precipitates as SiO_2, which combines with FeO and then forms a separate phase called fayalite (Fe_2SiO_4). Its melting point is about 1173°C and at this temperature, liquid Fe_2SiO_4 penetrates irregularly into FeO and the steel matrix. It is difficult to completely remove the FeO layer after descaling due to the very high strength of the eutectic compound Fe_2SiO_4/FeO. The remaining FeO scale is oxidized into red Fe_2O_3 during the subsequent cooling process. When steel contains more than 0.5 wt.% silicon, red scale normally occurs [9]. Red scale has a close relationship with silicon according to above researches. Therefore, more studies on the effect of silicon on the oxidation behavior of silicon-containing steels were conducted. Liu et al. [8] investigated the scale morphology of Fe-1.5 Si alloys and illustrated two forms of silicon distribution, i.e., granular silicon oxide precipitation in the iron matrix and a silicon-enriched phase, Fe_2SiO_4, located in the interface between the innermost oxide scale layer and the iron matrix. The relationship between silicon content and Fe_2SiO_4 morphology was expounded by Yuan et al. [10]. They found that Fe_2SiO_4 appeared as a net-like form in the innermost oxide scale layer close to iron matrix when the silicon content was 1.21 wt.%. However, no obvious net-like Fe_2SiO_4 was observed when the silicon content was less than 0.25 wt.%.

Several studies [11-13] proved that the mass gain of low-silicon steel is greater than that of high -silicon steel at temperatures below 1173°C (the melting point of fayalite). This is due to SiO_2 and solid Fe_2SiO_4 hindering the oxidation reaction, and increasing with increased silicon content. However, two opposing results have been obtained regrading the mass gain of silicon-containing steels at temperatures above 1173°C. Fukagawa et al. [7] and Suarez et al. [12,13] conducted similar experiments in which the binary oxidizing atmosphere was introduced during the isothermal process. They reported that the oxidation rate and the total mass gain increased with increasing silicon content. Similar results were obtained by Mouayd et al. [14] and Li et al. [15]. However, in previous study by Yuan et al. [10], a heating procedure, similar to that used in the industrial reheating furnaces during hot-rolled strip production, was designed where the binary oxidizing atmosphere was pumped from the beginning of the heating process. It was found that the mass gain of silicon-containing steels decreased with increasing silicon content at a temperature of 1260°C. The main reason for the difference in these results is that two different heating procedures were adopted. For practical application, the heating procedure similar to that used in the industrial reheating furnace in hot-rolled strip production is more meaningful. Therefore, in order to further clarify the effect of silicon content on the mass gain at high temperatures under heating procedures similar to those in industrial reheating furnaces, the effects of oxygen concentration and oxidation time on the oxidation behavior of silicon-containing steel are investigated in the present study.

* WUHAN UNIVERSITY OF SCIENCE AND TECHNOLOGY, THE STATE KEY LABORATORY OF REFRACTORIES AND METALLURGY, WUHAN, CHINA
** WUHAN UNIVERSITY OF SCIENCE AND TECHNOLOGY, KEY LABORATORY FOR FERROUS METALLURGY AND RESOURCES UTILIZATION OF MINISTRY OF EDUCATION, WUHAN, CHINA;
# Corresponding author: xuguang@wust.edu.cn

2. Materials and methods

2.1. Oxidation tests

Two steels (HS1.21: high silicon; LS0.25: low silicon) with different silicon contents were used. The chemical compositions are shown in Table 1. The materials were taken from a commercially produced hot strip (WISCO, China) 3 mm in thickness. The oxidation tests were conducted with a Setaram Setsys Evo Simultaneous Thermal Analyzer (STA, Setaram, Lyon, France) and the live changes in oxidation mass gain were fully recorded. The accuracy of temperature measurement is ±0.5°C, so that the effect of thermal drifts of thermobalance setup on mass gain can be ignored. Samples with dimensions of 15 mm × 10 mm × 3 mm were cut from the hot strip. A 4 mm diameter hole was drilled near the end of each specimen to suspend them during the oxidation tests. In addition, before the oxidation tests, the surfaces of all of the samples were polished to remove scale, thereby ensuring consistent surface conditions for all samples and avoiding the effects of surface impurities.

TABLE 1

Chemical compositions of two tested steels (wt.%)

Steel	C	Si	Mn	P	S	Al	Fe
HS1.21	0.069	1.21	1.40	0.010	0.001	0.035	Balance
LS0.25	0.071	0.25	1.37	0.011	0.001	0.031	Balance

Figure 1 shows the heating procedure. The samples were reheated to 1260°C by a segmented heating route, then held for 10 or 40 minutes, this was followed by cooling to room temperature at a rate of 50°C/min. The heating rates were 6.92°C/min from 0°C to 850°C and 3.15°C/min from 850°C to 1260°C, respectively. For practical application, the segmented heating route was based on the heating procedure used in industrial production. The total heating time was the same and the heating rates at different heating stages were dependent on the end temperature in the different heating sections. During the heating and isothermal holding periods, four kinds of binary gases with different oxygen concentrations were introduced into the STA chamber. The oxidizing atmospheres were 1.0% O_2 + 99.0% N_2, 2.0% O_2 + 98.0% N_2, 3.0% O_2 + 97.0% N_2, 4.0% O_2 + 96.0% N_2, (vol.%), respectively. In addition, an isothermal holding time of 90 minutes was used for all oxygen concentrations except 1.0% O_2 + 99.0% N_2. During the cooling period, an atmosphere of 21.0 vol% oxygen and 79.0 vol.% nitrogen was added to all samples to simulate the cooling process in air. Weight change during the oxidation period was continuously recorded.

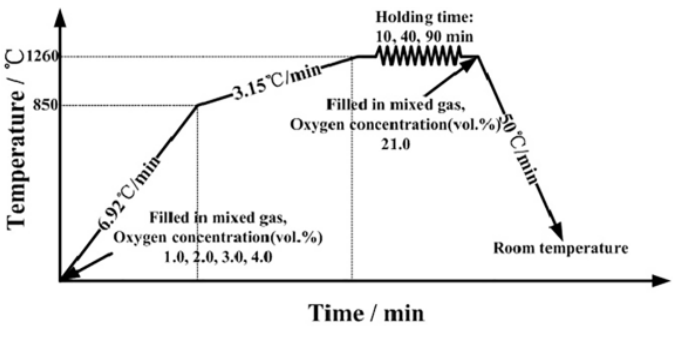

Fig. 1. The heating procedure

2.2. Oxide scale analyses

After oxidation, all samples were cold molded in resins at room temperature to protect the integrity of the oxide scale. Metallographic preparation, i.e., grinding, polishing, and washing with ethanol solution, was performed [16]. The morphology and composition of the oxide scale were analyzed using backscattered electron detection (BSED, FEI, Hillsboro, OR, USA) and energy-dispersive spectroscopy (EDS, OIMS, Oxford, UK) on a Nova 400 Nano scanning electron microscope (SEM, FEI, Hillsboro, OR, USA) operated at an accelerating voltage of 20 kV. X-ray diffraction (XRD, Panalytical, Almelo, the Netherlands) with Cu Kα radiation was also used to analyze the phase of the oxide scale under the following conditions: acceleration voltage, 40 kV; current, 150 mA; step, 0.06°. The XRD powder sample was scraped from the oxidized sample. In addition, the Image-Pro plus 6.0 software (Media Cybernetics, Rockville, MD, USA) was applied to measure the areas of Fe_2SiO_4 in unit widths. First, the total area of Fe_2SiO_4 in the inner layers was measured by color aberration using the software. Then, the total areas were divided by the width of the measured images to obtain the areas of Fe_2SiO_4 in unit widths [10]. The measured area can represent the amount of Fe_2SiO_4.

3. Results and discussions

3.1. Oxide scale composition

The energy spectrum diagram and XRD results from the oxide scale in HS1.21 steel oxidized in 2.0 vol.% oxygen concentration with an isothermal holding time of 40 min were used to determine the phases in each layer of the oxide scale. The morphology of oxide scale and the energy spectrum diagram points are presented in Fig. 2. Table 2 gives the corresponding main atomic percentages of each oxide scale layer according to Fig. 2. The atomic ratios of Fe/O in the outermost and middle layers are approximately 2/3 and 1/1, respectively. The atomic ratio of Fe/Si/O in the inner layer is about 2/1/4. The corresponding XRD results of the oxide scale are shown in Figure 3, in which no silicon is detected because it is difficult to scrape the inner layer scale containing silicon from the matrix surface. Based on the EDS and XRD results, four phases were determined Fe_2O_3, Fe_3O_4, Fe_2SiO_4 and FeO. The oxide scales of HS1.21 and LS0.25 are mainly the same constitution according to previous studies [17-20]. Therefore, the oxide scales of HS1.21 and LS0.25 can be said to mainly consist of three different layers, i.e., an upper layer Fe_2O_3, a middle FeO+Fe_3O_4 layer, and an inner FeO/Fe-

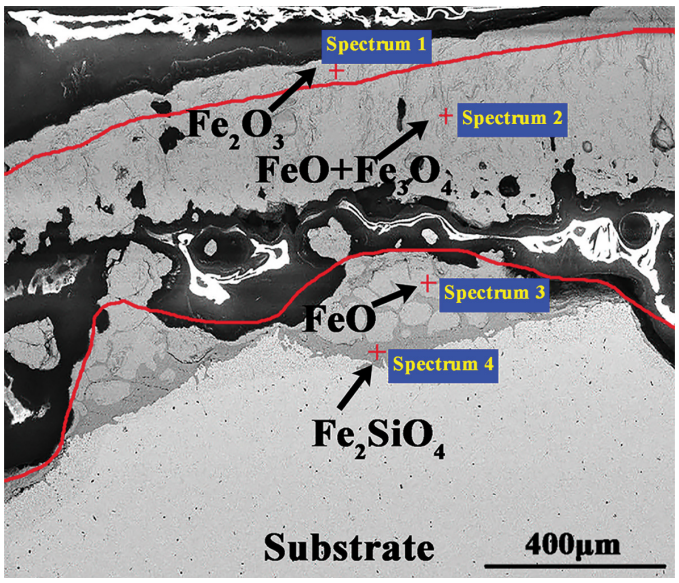

Fig. 2. Composition of the oxide scale formed in HS1.21 steel oxidized in 2.0 vol.% oxygen concentration with an isothermal holding time of 40 min

TABLE 2

The main atomic percentages in each layer of the oxide scale formed in HS1.21 steel oxidized in 2.0 vol.% oxygen concentration with an isothermal holding time of 40 min (atom %)

	Upper layer (Fe_2O_3)	Middle layer ($FeO+Fe_3O_4$)	Inner layer ($FeO+Fe_2SiO_4$)	
	Spectrum 1	Spectrum 2	Spectrum 3	Spectrum 4
O	57.68	55.80	54.72	54.69
Si	—	—	—	12.69
Mn	0.46	0.65	0.76	0.89
Fe	41.86	43.35	44.52	31.73

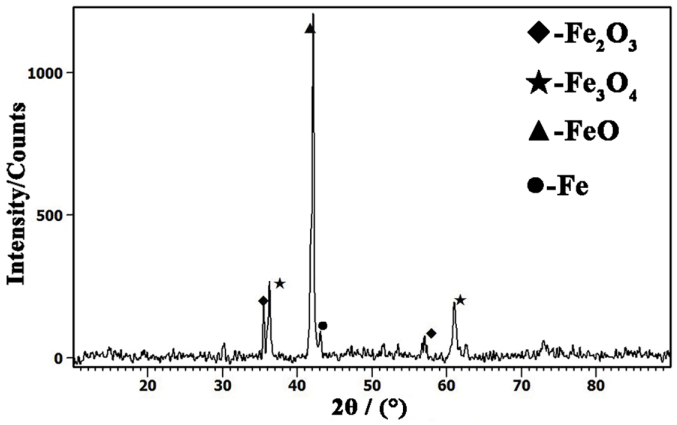

Fig. 3. X-ray diffraction pattern of oxide scale for HS1.21 steel oxidized in 2.0 vol.% oxygen concentration

$_2SiO_4$ layer. The net-like phase close to the scale-metal interface is a mixture of Fe_2SiO_4 and FeO, where dark gray (spectrum 4) is Fe_2SiO_4 and the light gray (spectrum 3) is FeO.

3.2. The morphology and amount of Fe_2SiO_4 in different oxygen concentrations

Fig. 4 shows the morphologies of Fe_2SiO_4 in steels containing different silicon contents and oxidized under various oxygen concentrations. It can be seen that the eutectic FeO/Fe_2SiO_4 forms primarily in the interface between the matrix and the scale, and irregularly penetrates into FeO and the matrix. The Fe_2SiO_4 phase is distributed in a net-like form and intensively bonds the iron matrix with FeO [21]. For the two steels, the Fe_2SiO_4 phase distributed in a net-like form when the oxygen concentration was

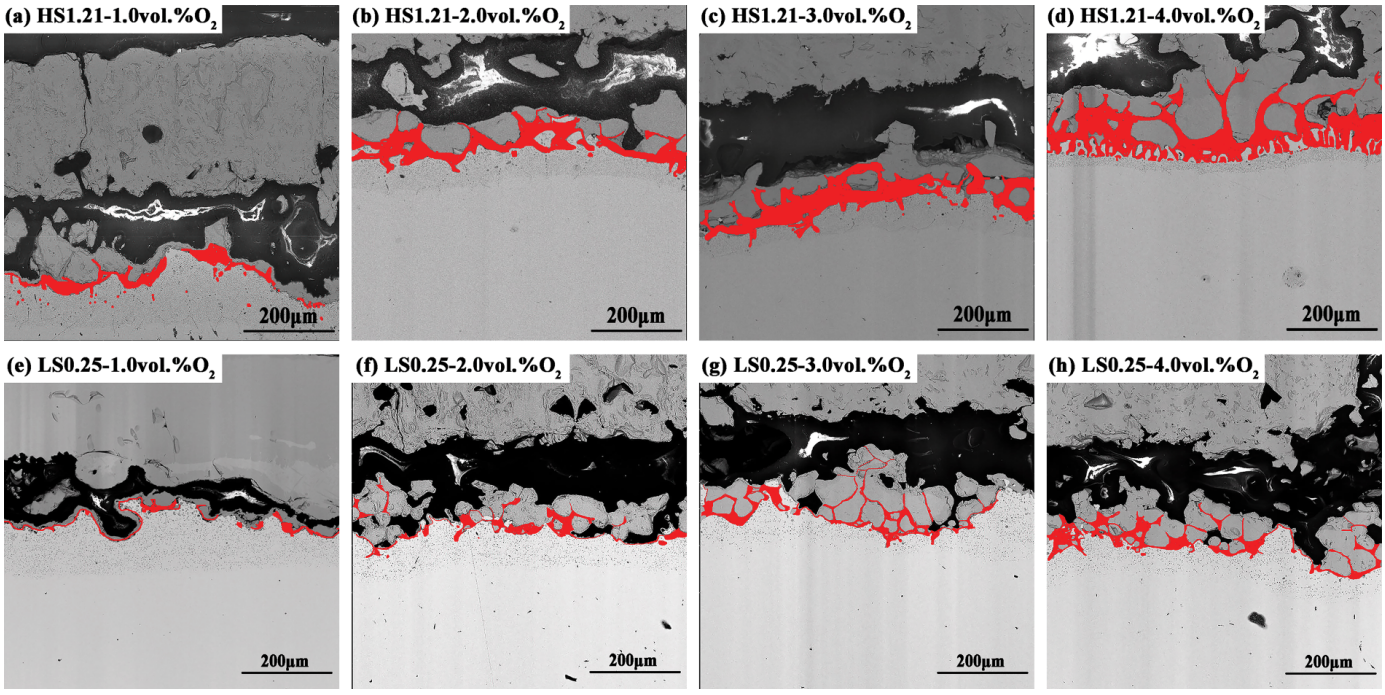

Fig. 4. The morphologies of Fe_2SiO_4 in steels containing different silicon contents oxidized at various oxygen concentrations

≥2.0 vol.%. In addition, the net-like Fe_2SiO_4 becomes more obvious with increasing oxygen concentration. The reasons for this net-like distribution of Fe_2SiO_4 have been reported in references [22,23]. The Pilling-Bedworth Ratio (PBR) is the ratio of oxide volume and consumed metal volume. The PBR of iron oxide or silicon oxide is more than 1 because the oxide volume is greater than that of the consumed metal, leading to a compressive stress in the oxide. The compressive stress at the oxide layer/metal interface is larger than at the outer position, resulting in the pressure differences at different places of the scale. The pressure difference in the liquefied Fe_2SiO_4 phase at a temperature of 1260°C forces a part of Fe_2SiO_4 to permeate into the inner scale. The liquid Fe_2SiO_4 phase distributes along FeO grain boundaries and the net-like Fe_2SiO_4 phase forms after its solidification.

The areas of Fe_2SiO_4, in unit widths of steels, containing different silicon contents oxidized at various oxygen concentrations with an isothermal holding time of 40 min are given in Fig. 5. The results indicate that the amount of Fe_2SiO_4 increased with increasing silicon content and oxygen concentration. Moreover, with increasing oxygen concentration, the increase in Fe_2SiO_4 amount in HS1.21 steel was faster than that in LS0.25 steel.

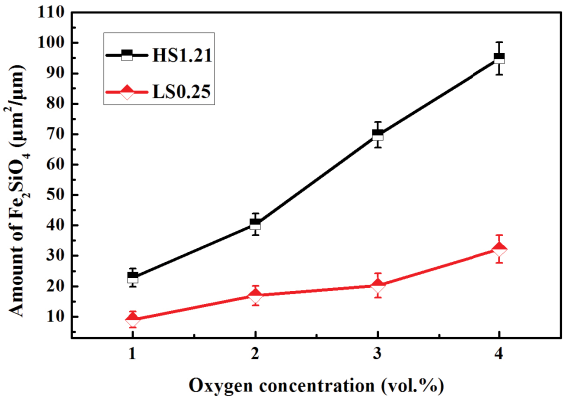

Fig. 5. Fe_2SiO_4 areas in unit widths in steels containing different silicon contents oxidized at various oxygen concentrations

3.3. Oxidation kinetics

Fig. 6 presents the total mass gain per unit surface of samples oxidized under various oxygen concentrations, and the isothermal holding times are all 40 minutes. This indicates that the total mass gain not only increased with increasing oxygen concentration, but also increased with decreasing silicon content. It is generally acknowledged that the oxidation reaction is controlled by the ions required for the formation of oxide scale. The combination and diffusion among ions are not only dependent on the amount of ions, but also are related with the oxidation temperature. According to Fick's law, the diffusion flux of ions is proportional to the diffusion coefficient, and the diffusion coefficient is an exponential function of temperature. Therefore, when the temperature and the amount of oxygen in a unit surface area of sample increase, the combination and diffusion among ions increase heavily, resulting in an increased oxidation mass gain. Moreover, the total mass gain increases with decreasing silicon content. This can be attributed to the inhibition effects of Fe_2SiO_4, which play a dominant role during the entire oxidation reaction. For LS0.25 steel, the amount of SiO_2 and solid Fe_2SiO_4 is smaller due to the low silicon content. The inhibition effects of SiO_2 and solid Fe_2SiO_4 [24,25] on the oxidation reaction are smaller than that in HS1.21 steel, resulting in an earlier start to the intense oxidation stage. This leads to a longer high-temperature oxidation of LS0.25 steel [10,26]. Therefore, the mass gain of LS0.25 steel is greater than that of HS1.21 steel during an isothermal holding time of 40 minutes. The ordinate represents for the oxidation mass gain per unit surface of sample, so the differences in the column heights are small. But the results in Figure 6 demonstrate the greater mass gain of LS0.25 steel.

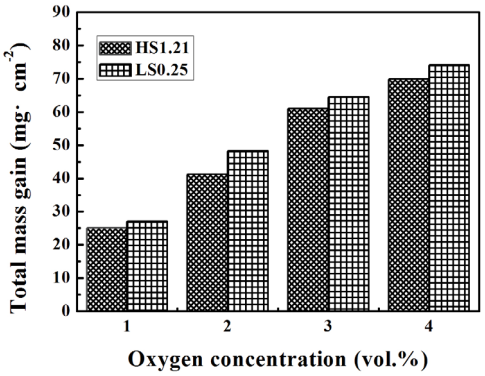

Fig. 6. The total mass gains of two different steels with an isothermal holding time of 40 minutes

Fig. 7 shows the total mass gain per unit surface of samples oxidized in various oxygen concentrations, except 1.0 vol.%; the isothermal holding times were all 90 minutes. It can be seen that when the isothermal holding time is 90 minutes, the total mass gain per unit surface of LS0.25 steel is larger than that of HS1.21 steel at an oxygen concentration of 2.0 vol.%. Whereas, the total mass gain of LS0.25 steel is smaller when the oxygen concentration ≥2.0 vol.%. This indicates that the effect of silicon content on the total mass gain depends on both the oxygen concentration and oxidation time. The differences in column heights are also small, but reflect the change trend in mass gain as the difference percentages in column height are calculated to be 8.5%, 8.1% and 7.1% for oxygen concentrations of 2.0, 3.0 and 4.0 vol.%.

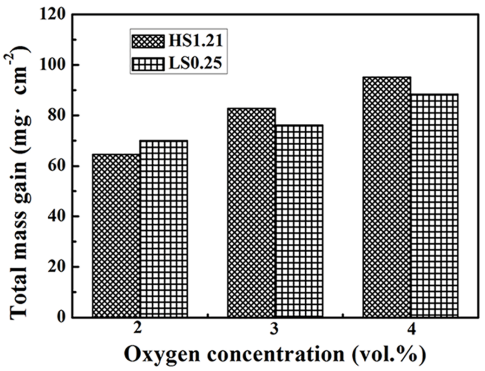

Fig. 7. The total mass gains of two different steels with an isothermal holding time of 90 minutes

Fig. 8 gives the representative fitting results of the oxidation mass gain versus time for HS1.21 and LS0.25 steels oxidized in 4.0 vol.% oxygen with an isothermal holding time of 40 min. According to Kofstad [27], an oxidation process of silicon-containing steel obeying linear, parabolic or cubic law is generally expressed as:

$$\Delta W^n = K_T \cdot t \tag{1}$$

where, ΔW is the mass gain per unit area at time t, mg·cm^{-2}; n is a constant having values of 1, 2 or 3 for linear, parabolic, and cubic rate laws, respectively; K_T is the oxidation rate constant (K_L (mg·cm^{-2}·min^{-1}) for the linear part and Kp (mg^2·cm^{-4}·min^{-1}) for the parabolic part) at constant temperature T; and t is oxidation time at T, min. The values of n can be obtained to be $n = 1$ for HS1.21 steel and $n = 1.86$ for LS0.25 steel, separately. Therefore, the mass gain versus time follows an almost linear relationship in HS1.21 steel, whereas it is a near parabolic relationship in LS0.25 steel.

The oxidation mass gain versus time curves of HS1.21 and LS0.25 steels oxidized in 4.0 vol.% oxygen are shown in Fig. 9a. These results represent real oxidation phenomena with time. It can be seen that mass gain versus time follows an almost linear relationship (as shown in Fig. 8a) in HS1.21 steel regardless of the holding time, whereas in LS0.25 it follows a near parabolic relationship (as shown in Fig. 8b). The oxidation reaction is controlled primarily by two opposing factors, i.e., the promotion effect of the liquefied FeO/Fe_2SiO_4 on ions diffusion and the inhibition effect of the oxide scale on ions diffusion. At temperatures higher than the melting point of Fe_2SiO_4, the amount of liquid Fe_2SiO_4 increases with time and silicon content, and enhances the promotion effect (as shown in Fig. 4). Simultaneously, the oxide scale becomes thicker with time, resulting in deceleration of the oxidation reaction. For HS1.21 steel, the subsequent oxidation reaction follows a nearly linear relationship after the intense oxidation point (point A), suggesting that the promotion and inhibition effects on ion diffusion reach a dynamic equilibrium [10]. As the oxygen concentration is higher (4.0 vol.%), more liquid Fe_2SiO_4 forms and acts as a diffusion passage. The increase in the promotion effect by liquid Fe_2SiO_4 on ions diffusion is accompanied by an increase in oxide scale. The oxidation rate remains constant when the two opposite effects reach dynamic equilibrium. However, the total mass gain versus time follows a near parabolic relationship in LS0.25 steel, indicating that the inhibition effect of oxide scale on ions diffusion plays a leading role. This is because of the smaller amount of liquid Fe_2SiO_4 in LS0.25 steel due to the lower silicon content, even in high oxygen concentrations (as shown in Fig. 4). Therefore, the promotion effect by liquid Fe_2SiO_4 on ions diffusion is small. With increasing isothermal holding time, more oxidation mass gain appears and the inhibition effect of the oxide scale increases. As a consequence, the oxidation rate decreases with time, and mass gain versus time follows a near parabolic relationship.

In addition, the linear oxidation rate constant K_L of HS1.21 steel oxidized in an oxygen concentration of 4.0 vol.% during

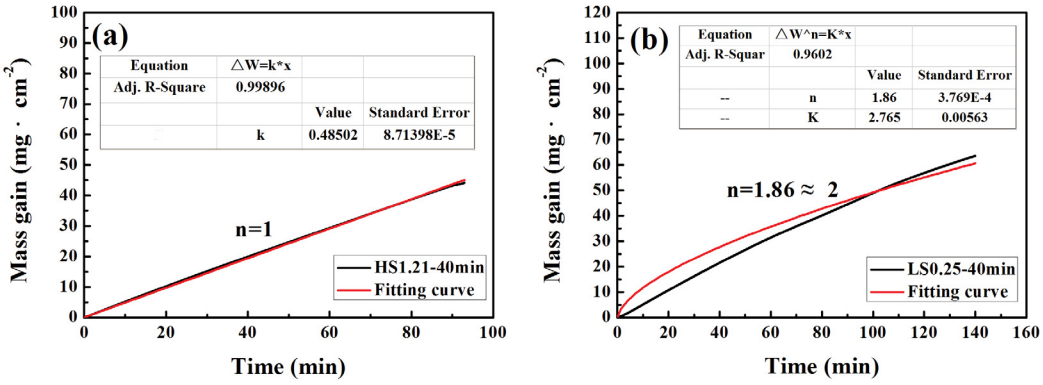

Fig. 8. The fitting results of the oxidation mass gain versus time of HS1.21 and LS0.25 steels oxidized in 4.0 vol.% oxygen with an isothermal holding time of 40 min

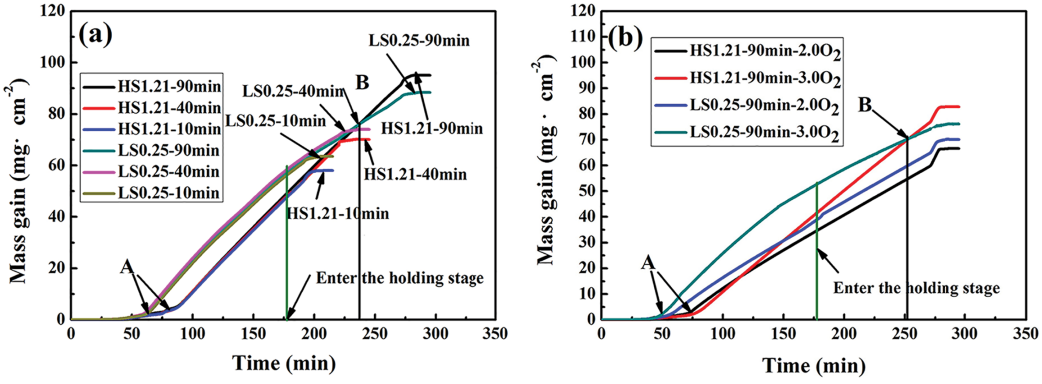

Fig. 9. Oxidation mass gain versus time in different steels oxidized in oxygen (a) 4.0vol.% and (b) 2.0vol.% and 3.0vol.%

an isothermal holding period of 90 minutes is calculated to be 0.485 $mg \cdot cm^{-2} \cdot min^{-1}$ from equation (1). The linear oxidation rate constant is equal to the average oxidation rate. The average parabolic oxidation rate constant K_p of LS0.25 steel during an isothermal holding period of 90 minutes is calculated to be 2.765 $mg^2 \cdot cm^{-4} \cdot min^{-1}$. The oxidation rate of LS0.25 steel generally decreases with time (Fig. 9a). This means that the curves of mass gain in LS0.25 and HS1.21 steels will intersect at a certain holding time. At the cross point, the mass gain of HS1.21 steel is larger than that of LS0.25 steel. This cross point can be defined as the critical time point (point B: 236.54 min). The mass gain of low-silicon steel is larger before and smaller after the critical point. It should be noted that the values of K_L and K_p in the present study are different from those in literatures [11,14]. This may be attributed to two main reasons. At first, the chemical compositions of the tested steels in present study are obviously different from those in literatures [11,14], resulting in the different oxidation processes. Secondly, the heating procedure in the present study is similar to that used in the industrial reheating furnace in hot-rolled strip production, which is different from the procedures applied in the literatures [11,14].

The total mass gain versus time curves of HS1.21 and LS0.25 steels oxidized in 2.0 vol.% and 3.0 vol.% oxygen at an isothermal holding time of 90 minutes are given in Figure 9b. It can be seen that the curves for steels oxidized in 3.0 vol.% oxygen concentration intersect at 253.85 min. The critical time point in 3.0 vol.% oxygen concentration is later than that in 4.0 vol.%. In addition, mass gain versus time follows an almost linear relationship in both steels oxidized in 2.0 vol.% oxygen. The increase in oxide scale is reduced due to a lower oxygen concentration. The promotion effect by liquid Fe_2SiO_4 on ions diffusion and the inhibition effect of the oxide scale on ions diffusion reach dynamic equilibrium, resulting in a constant oxidation rate.

In summary, the experimental results indicate that the effect of silicon on mass gain depends on the oxygen concentration and the oxidation time. Previous studies have not considered these factors. In the present study, the oxygen concentration and oxidation time are taken into account, and the heating procedure applied is similar to that used in industrial reheating furnaces in hot-rolled strip production. Therefore, these results are more meaningful from a practical application viewpoint and provide references for practical application.

4. Conclusions

The combined influence of silicon content and oxygen concentration on the oxidation process of silicon-containing steel was investigated using four different oxygen concentrations and three different isothermal holding times. The results clarify that the effect of silicon on mass gain depends on the oxygen concentration and the oxidation time. The mass gain of low-silicon steel is greater than that of high-silicon steel at 1260°C in the oxygen concentrations of 1.0 vol.% and 2.0 vol.%, even when the isothermal holding time is 90 minutes. However, there is a critical time point for mass gain in oxygen concentrations ≥3.0 vol.%. The mass gain of low-silicon steel is greater before the critical point, and smaller after the critical point. The critical time is postponed with decreasing oxygen concentration.

Acknowledgments

The authors gratefully acknowledge the financial supports from the National Natural Science Foundation of China (NSFC) (No. 51274154).

REFERENCES

[1] H. Okada, T. Fukagawa, H. Ishihara, A. Okamoto, M. Azuma, Y. Matsuda, ISIJ Int. **80**, 849-854 (1994).
[2] A. Chattonpadhyay, T. Chanda, Scr. Mater. **58**, 882-885 (2008).
[3] X.Q. Xu, X.F. Zhang, X.Y. Sun, Z.P. Lu, Corr. Sci. **65**, 317-321 (2012).
[4] M. Takeda; T. Onishi. Mater. Sci. Forum. **522**, 477-488 (2006).
[5] B. He, G. Xu, M.X. Zhou, Q. Yuan, Metals. **6**, 137-145 (2016).
[6] H. Okada, T. Fukagawa, H. Ishihara, ISIJ Int. **35**, 886-891 (1995).
[7] T. Fukagawa, H. Okada, Y. Maeharara, ISIJ Int. **34**, 906-911 (1994).
[8] T. Fukagawa, H. Okada, Y. Maehara, H. Fujikawa, ISIJ Int. **82**, 63-68 (1996).
[9] X.J. Liu, G.M. Cao, Y.Q. He, T. Jia, Z.Y. Liu, J. Iron Steel Res. Int. **20**, 73-78 (2013).
[10] Q. Yuan, G. Xu, M.X. Zhou, B. He, Metals. **6**, 94-103 (2016).
[11] Y.L. Yang, C.H. Yang, S.N. Lin, C.H. Chen, W.T. Tsai, Mater. Chem. Phys. **112**, 566-571 (2008).
[12] L. Suarez, J. Schneider, Y. Houbaert, Defect Diffus. Forum. Trans Tech Publications, 661-666, Switzerland 2008.
[13] L. Suarez, J. Schneider, Y. Houbaert, Defect Diffus. Forum. Trans Tech Publications, 655-660, Switzerland 2008.
[14] A.A. Mouayd, A. Koltsov, E. Sutter, B. Tribollet, Mater. Chem. Phys. **143**, 996-1004 (2014).
[15] S.J. Li, Y.B. Liu, W. Zhang, Q.S. Sun, L.P. Wang, J. Iron Steel Res. Int. **27**, 55-60 (2015). (In Chinese).
[16] R. Logani, W.W. Smeltzer, Oxid. Met. **1**, 3-21 (1969).
[17] A. Rahmel, Corrons. Sci. **39**, 354 (1988).
[18] G.M. Cao, T.Z. Wu, R. Xu, Z.F. Li, F.X. Wang, Z.Y. Liu, J. Iron Steel Res. Int. **22**, 892-896 (2015).
[19] R.Y. Chen, W.Y.D. Yuen, Oxid. Met. **59**, 433-468 (2003).
[20] R.Y. Chen, W.Y.D. Yuen, ISIJ Int. **45**, 52-59 (2005).
[21] X.J. Liu, G.M. Cao, D.M. Nie, Z.Y. Liu, J. Iron Steel Res. Int. **20**, 54-59 (2013).
[22] G. Garnaud, R.A. Rapp, Oxid. Met. **11**, 193-198 (1977).
[23] R.W. Staettle, M.G. Fontana, Advances in Corrosion Science and Technology, Springer-Verlag, 239-356, New York 1974.
[24] A. Atkinson, Corros. Sci. **22**, 87-102 (1982).
[25] T. Adachi, G.H. Meier, Oxid. Met. **27**, 347-366 (1987).
[26] Q. Yuan, G. Xu, M.X. Zhou, B. He, Int. J. Miner. Metall. Mater. **23**, 1-8 (2016).
[27] P. Kofstad, J. Less Common Metals. **7**, 241-266 (1964).